The Egyptian Journal of Radiology and Nuclear Medicine (2016) 47, 859–865

Egyptian Society of Radiology and Nuclear Medicine

The Egyptian Journal of Radiology and Nuclear Medicine

www.elsevier.com/locate/ejrnm
www.sciencedirect.com

ORIGINAL ARTICLE

Semi-automatic detection and segmentation algorithm of saccular aneurysms in 2D cerebral DSA images

Nisreen Sulayman [a,*], **Moustafa Al-Mawaldi** [a], **Qosai Kanafani** [b]

[a] *Biomedical Engineering Department, Faculty of Mechanical and Electrical Engineering, Damascus University, Damascus, Syria*
[b] *Faculty of Mechanical and Electrical Engineering, Damascus University, Damascus, Syria*

Received 26 May 2015; accepted 24 March 2016
Available online 13 April 2016

KEYWORDS

Digital subtraction angiography;
Saccular aneurysms;
Image enhancement;
Image segmentation;
Shape features

Abstract *Objective:* To detect and segment cerebral saccular aneurysms (CSAs) in 2D Digital Subtraction Angiography (DSA) images.
Patients and methods: Ten patients underwent Intra-arterial DSA procedures. Patients were injected with Iodine-containing radiopaque material. A scheme for semi-automatic detection and segmentation of intracranial aneurysms is proposed in this study. The algorithm consisted of three major image processing stages: image enhancement, image segmentation and image classification. Applied to the 2D Digital Subtraction Angiography (DSA) images, the algorithm was evaluated in 19 scene files to detect 10 CSAs.
Results: Aneurysms were identified by the proposed detection and segmentation algorithm with 89.47% sensitivity and 80.95% positive predictive value (PPV) after executing the algorithm on 19 DSA images of 10 aneurysms. Results have been verified by specialized radiologists. However, 4 false positive aneurysms were detected when aneurysms' location is at Anterior Communicating Artery (ACA).
Conclusion: The suggested algorithm is a promising method for detection and segmentation of saccular aneurysms; it provides a diagnostic tool for CSAs.

1. Introduction

Medical image processing is the most challenging and emerging field now days (1). Digital Subtraction Angiography (DSA) has been the standard of reference for the detection and characterization of intracranial aneurysms (2). Cerebral saccular aneurysms (CSAs) are initially rounded, berrylike outpouchings that arise at a branching site on the parent artery (3), and more than 90% of the intracranial aneurysms are of this type (4). Fig. 1 shows an example of CSA which is located at the right middle cerebral artery.

Subarachnoid hemorrhage due to the rupture of an intracranial aneurysm is a devastating event associated with

* Corresponding author. Tel.: +963 955946675.
E-mail address: sulayman.nisreen@gmail.com (N. Sulayman).
Peer review under responsibility of The Egyptian Society of Radiology and Nuclear Medicine.

http://dx.doi.org/10.1016/j.ejrnm.2016.03.016

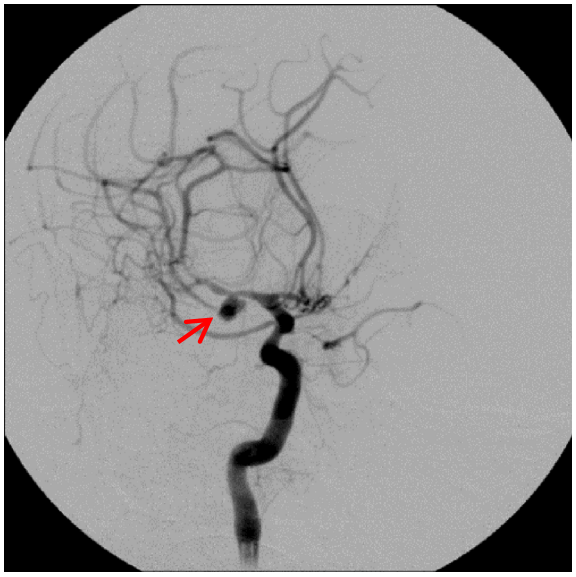

Fig. 1 2D cerebral DSA image with CSA at the right middle cerebral artery.

high rates of mortality (40–50%) and morbidity (5). At first glance, Aneurysms segmentation seems to be easy but the local inhomogeneous contrast agent distribution, patient movement as well as the smooth intensity ramp between blood vessels and background make it a difficult task (6).

Segmentation methods vary depending on the imaging modality, application domain, method being automatic or semi-automatic, and other specific factors. There is no single segmentation method that can extract vasculature from every medical image modality (7).

Intracranial vessels and aneurysms segmentation algorithms can be divided into several categories: Pattern recognition techniques, Model-based approaches, Tracking-based approaches, Artificial Intelligence-based approaches and hybrid approaches.

Pattern recognition techniques deal with the automatic detection or classification of objects or features. For vessel extraction, pattern recognition techniques are concerned with the automatic detection of vessel structures and features. Pattern recognition techniques include seven categories: (1) multiscale approaches (8), (2) skeleton-based (centerline) approaches (9,10), (3) ridge-based approaches (11,12), (4) region growing approaches (13,14), (5) differential geometry-based approaches (15,16), (6) matching filters approaches (17,18), and (7) mathematical morphology schemes (19).

Model-Based (MB) Approaches apply explicit vessel models to extract the vasculature. MB approaches are divided into four categories: (1) deformable models (20), (2) Parametric models (21), (3) Template matching (22), and (4) Generalized cylinders (23). Active contour models or snakes are a special case of a more general technique of matching a deformable model by means of energy minimization (7).

Tracking-Based Approaches apply local operators on a focus known to be a vessel and track it. On the other hand, patter recognition approaches apply local operators to the whole image. Vessel tracking (VT) approaches, starting from an initial point, detect vessel centerlines or boundaries by analyzing the pixels orthogonal to the tracking direction. Different methods are employed in determining vessel contours or centerlines. Edge detection operation followed by sequential tracing by incorporating connectivity information is a straightforward approach (7). Fuzzy clustering is an approach to identifying vessel segments. It uses linguistic descriptions such as "vessel" and "nonvessel" to track vessels in retinal angiogram images (24).

Artificial Intelligence-Based Approaches (AIBA) utilize knowledge to guide the segmentation process and to delineate vessel structures. Different types of knowledge are employed in different systems from various sources. One knowledge source is the properties of the image acquisition technique, such as Digital Subtraction Angiography (DSA) and computed tomography (CT). Some applications utilize a general blood vessel model as a knowledge source (7).

Hybrid approaches combine one method or more of the aforementioned approaches to segment vessel structure. For instance, Hu and Hoffman (25) extracted the object boundaries by combining an iterative thresholding approach with region growing and component label analysis.

Existing approaches for vessel structures segmentation have the following limitations (26):

1. Some approaches require user interaction to initialize a vessel of interest (27,28).
2. Some deformable models assume circular vessel cross sections; this holds for healthy people, but not for patients with a stenosis or an aneurysm (29).
3. Some approaches are computationally expensive (30).

Despite the availability of many image segmentation methods, with varying approaches and algorithms, there is no dominant method in terms of effectiveness, across all areas (31). The segmentation of cerebral vasculature with aneurysms is a difficult task often due to their complex geometry as well as limited image contrast and spatial resolution, which are critical factors compared with the size of these vascular segments (32).

In this paper, CSAs are detected and segmented semi-automatically from 2D cerebral DSA images through two steps. First, potential regions of interest (potential aneurysms) are detected by pre-processing the DSA images, segmenting the vessel tree, and applying morphological processing. Second, false positive reduction method is applied on the areas highlighted in the first step, where the reduction scheme depends on the extracted features of the potential aneurysms.

2. Patients and methods

2.1. Patients

This study was approved by Damascus University and Al-Assad University hospital in Damascus/Syria. There were 6 female and 4 male patients, and their ages ranged from 38 to 64 years, with a mean age of 47.2 ± 7.7 years. Patients were clinically diagnosed for cerebral saccular aneurysms. Table 1 shows demographic characteristics of the studied patients.

2.2. DSA protocol

DSA imaging was performed by DSA modality station (Siemens/AXIOM-Artis), DSA consisted of an X-ray assembly

Table 1 Demographic characteristics of the studied patients.

Total number	10	
Age		
(Mean ± SD)	47.2 ± 7.7	
Range	38–64	
Female/Male	6/4	
Clinical presentation	Cerebral saccular aneurysms	
Location of aneurysms		
	Anterior Communicating Artery (ACA)	5
	Left Internal carotid artery (LICA)	2
	Right Internal carotid artery (RICA)	1
	Right Middle cerebral artery (RMCA)	1
	Posterior communicating artery (PCA)	1

and an image intensifier, and both are mounted on Floor-Mounted C-arm. Patients were injected with Iodine-containing radiopaque material. Contrast material is delivered by a small catheter placed superselectively in the cerebral arteries: left/right internal carotid artery or left/right vertebral artery. Lateral and/or oblique projections were chosen with different angles for each patient.

2.3. Medical image processing

In this study, 19 cerebral DSA scene files of 10 patients were used to extract images of cerebral blood vessels. The image's dimensions were 512×512 with bit depth equal to 8 in the range [0–255], and pixel size was 0.34 mm. Pre-contrast and post-contrast images of different patients have been chosen manually from each 3D time-series for the study.

Pre-contrast images are images without contrast material, and post-contrast images are images that best depict the blood vessels. The images represent transition of the contrast material during time intervals through the cerebral blood vessels; the manual selection of frames has been done to minimize patient's motion artifacts between frames during contrast material transition.

Fig. 2 shows the flowchart of the semi-automatic detection and segmentation algorithm of CSAs in cerebral DSA images. The algorithm includes three major image processing steps: image enhancement, image segmentation and image classification.

Processing starts by enhancing cerebral DSA images in order to reduce noise by applying a spatial Gaussian low pass filter of kernel-size 3 with sigma 0.5 to the pre-contrast image to reduce noise while retaining edges present in the image followed by calculating the subtraction image between the pre-contrast and post-contrast images. After that, a Frangi filter is applied to the subtraction image to emphasize vessel-like structures. Intensity inhomogeneity has been corrected using custom filter of kernel-size 5, and it is a weighted average filter with different coefficients giving more importance (weight) to the pixel at the center; the other pixels are inversely weighted as a function of their distance from the center of the filter and the diagonal pixels are weighted less than the immediate neighbors of the center of the filter. Fig. 3 shows image enhancement stage. Fig. 3a shows cerebral DSA image.

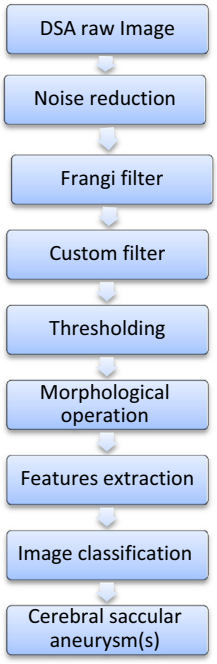

Fig. 2 The flowchart of the algorithm for semi-automatic detection and segmentation of saccular aneurysms in cerebral DSA images.

Fig. 3b shows cerebral DSA image enhanced using a Frangi filter. Fig. 3c shows cerebral DSA image enhanced using a custom filter.

After enhancing cerebral DSA images, image segmentation was done by thresholding using Otsu's method. The result is shown in Fig. 4a. After that, the largest connected component in the binary image which represents the vessel tree has been selected depending on region properties after removing all regions separated from it. The result is shown in Fig. 4b. Morphological processing starts by eroding the binary image with a disk structuring element with small radius to refine the segmentation.

To detach the CSA, opening and closing morphological operations have been applied, and first we apply opening morphological operation followed by closing using the same disk structuring element with a suitable radius, then opening operation has been done using a disk structuring element with larger radius than the first time. To get rid of small minor blood vessels which may be still attached to cerebral saccular aneurysms in some cases, image erosion followed by dilation using line structuring elements with two angels "0" and "90" has been used. The final result of morphological operations is shown in Fig. 4c which shows that false positive aneurysms beside the true one (red arrow) have been detected and they need a special processing to get rid of them. Removing false positive aneurysms has been achieved through several steps.

Processing starts by removing objects whose area is less than certain empirical value. This value has been selected after studying a set of cerebral DSA images. The result is shown in Fig. 5a. Connected component labeling has been used to label each component in the binary image; the result is shown in Fig. 5b. After that, shape features extraction has been done.

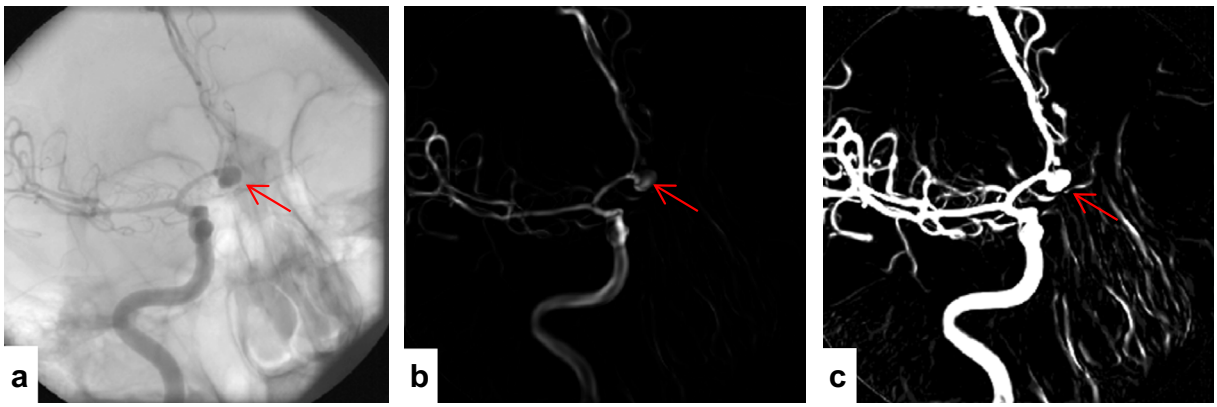

Fig. 3 Image enhancement stage. (a) Cerebral DSA image with saccular aneurysm (red arrow), (b) enhanced cerebral DSA image using Frangi filter and (c) cerebral DSA image after using a custom filter.

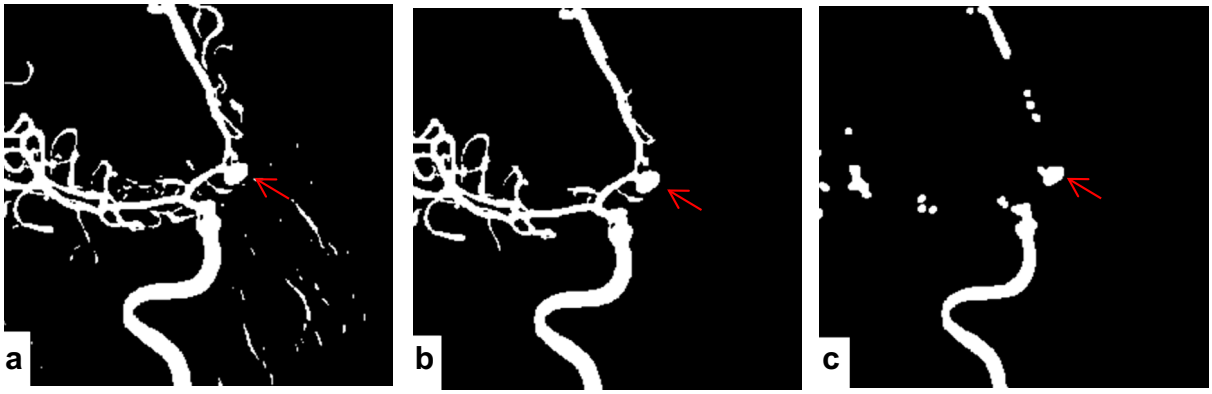

Fig. 4 (a) Segmented image using Otsu's method. (b) Vessel tree. (c) Morphological operations result.

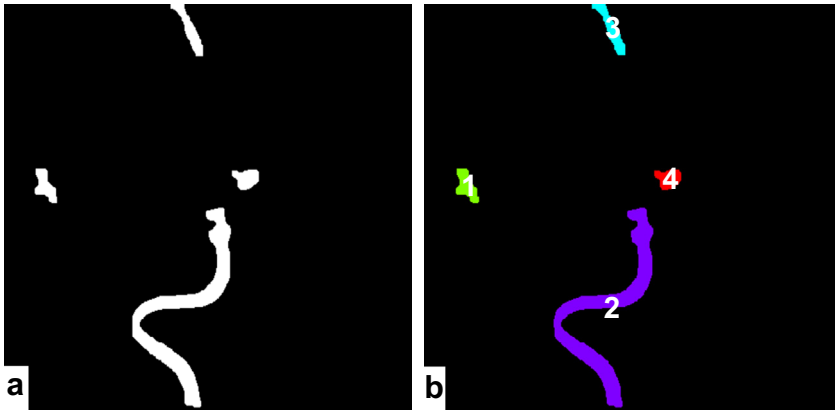

Fig. 5 (a) Result of removing objects whose areas are less than an empirical value. (b) Labeled connected component.

We have used Rule-based classification using shape features to perform image classification. Shape features include circularity, solidity, and eccentricity. Circularity is defined by next equation; solidity is defined by the proportion of the pixels in the convex hull that are also in the region; and eccentricity is a scalar that specifies the eccentricity of the ellipse that has the same second-moments as the region. It is the ratio of the distance between the foci of the ellipse and its major axis length, an ellipse whose eccentricity is 0 is actually a circle.

$$C = P^2/(4 * \pi * A) \quad (1)$$

where

C: circularity.

P: perimeter; the distance around the boundary of the region.

A: area; actual number of pixels in the region.

Table 2 shows objects' shape features according to their labels in Fig. 5b. Features include circularity, solidity and

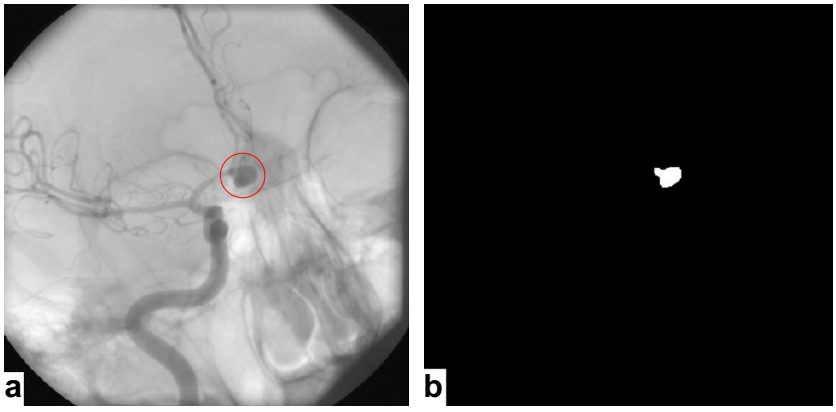

Fig. 6 (a) Saccular aneurysm detection in cerebral DSA image. (b) Segmented aneurysm.

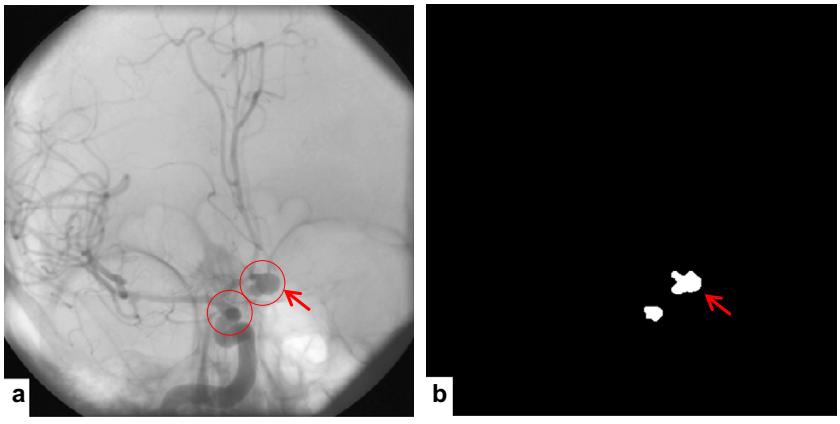

Fig. 7 (a) False positive aneurysm is detected in addition to the true one (red arrow). (b) Segmented True positive aneurysm (red arrow) beside the False one.

Table 2 Blobs' properties according to their labels in Fig. 5b.

Blob number	Circularity	Solidity	Eccentricity
#1	1.73	0.79	0.90
#2	7.23	0.35	0.91
#3	2.54	0.79	0.99
#4	1.25	0.92	0.65

eccentricity. Empirical shape features values are determined by computing some statistics on extracted features of the potential aneurysms, and an object is classified to be an aneurysm when circularity $\leqslant 1.6$, solidity $\geqslant 0.8$, and eccentricity $\leqslant 0.85$.

3. Results and discussion

The proposed algorithm to detect and segment CSAs from other structures that are present in cerebral 2D DSA images has been tested on 19 cerebral DSA scene files of 10 cerebral saccular aneurysms: five CSAs located at anterior communicating artery of five patients, two CSAs located at left internal carotid artery of two patients, and one CSA at each of the following sites: posterior communicating artery, right internal carotid artery, and right middle cerebral artery.

Cerebral saccular aneurysms were identified by the proposed detection and segmentation algorithm with 89.47% sensitivity and 80.95% positive predictive value (PPV) on DSA data. These results were obtained by computing the following quantities: number of true positive aneurysms (TPA), number of false positive aneurysms (FPA), and number of false negative aneurysms (FNA). The calculated values of TPA, FPA and FNA are 17, 4 and 2 respectively after executing the algorithm on 19 DSA images of 10 aneurysms. Sensitivity and positive predictive value are defined as (33)

$$\left.\begin{aligned}\text{Sensitivity} &= \frac{\text{TPA}}{\text{TPA+FNA}} \times 100\% \\ \text{Positive predictive value} &= \frac{\text{TPA}}{\text{TPA+FPA}} \times 100\%\end{aligned}\right\} \quad (2)$$

Fig. 6a shows DSA image with red circle about the aneurysm as a result of detection and Fig. 6b shows the segmented aneurysm. Fig. 7 shows an example of false positive CSA result in addition to the true one.

Visual inspection has been used as the only validation method to judge aneurysm separation from the rest of the vessel tree (34). Visual inspection has been verified by three specialized radiologists who insured the correct detection and segmentation of CSAs of cerebral DSA images. Radiologists had been also interested in the false positive results as it might need more investigation during clinical inspection as they are potential candidate regions of CSA.

4. Conclusion

Semi-automatic algorithm for detection and segmentation of cerebral saccular aneurysms in 2D DSA images has been developed. It could properly handle the intensity variation within vessel regions to perform a smooth segmentation. The algorithm returns few false positive aneurysms and does not involve a complex false positive reduction scheme. The sensitivity of algorithm is 89.47% and positive predictive value is 80.95%. Algorithm could be developed to have a computer aided diagnosis of cerebral saccular aneurysms to assist radiologists' image interpretation as a "second opinion" (35–37) and results could be used for advanced analysis in content based image retrieval (CBIR) as segmentation is considered one of the first and important steps (38). As future work we plan to enlarge DSA images database and perform additional steps with the proposed approach by extending the features used to reduce false positive aneurysms.

Conflict of interest

There is no conflict of interest to declare.

Acknowledgements

The authors of this paper would like to thank Al-Assad University Hospital in Damascus/Syria and the stuff of Radiology department for their cooperation in getting the data. Special thanks to the radiologists: Mr. Tayseer Al-meeri, Mr. Khaldoon Al-jammaz and Professor Yousef Al-berro who validated the results.
Authors would like to express their sincere thanks and appreciation to Mr. Lambert Zijp from the Netherlands Cancer Institute-Division of Radiotherapy who gave much to this paper.

References

(1) Pandey ON, Jogi SP, Yadav S, Arjun V, Kumar V. Review on brain tumor detection using digital image processing. Int J Sci Eng Res 2014;5(5):1351–5.
(2) Villablanca JP, Jahan R, Hooshi P, Lim S, Duckwiler G, Patel A, et al. Detection and characterization of very small cerebral aneurysms by using 2D and 3D helical CT angiography. Am J Neuroradiol 2002;23(7):1187–98.
(3) Satoh T, Omi M, Ohsako C, Katsumata A, Yoshimoto Y, Tsuchimoto S, et al. Influence of perianeurysmal environment on the deformation and bleb formation of the unruptured cerebral aneurysm: assessment with fusion imaging of 3D MR cisternography and 3D MR angiography. Am J Neuroradiol 2005;26(8):2010–8.
(4) Campo-Deaño L, Oliveira MS, Pinho FT. A review of computational hemodynamics in middle cerebral aneurysms and rheological models for blood flow. Appl Mech Rev 2015;67(3).
(5) Millán RD, Dempere-Marco L, Pozo JM, Cebral JR, Frangi AF. Morphological characterization of intracranial aneurysms using 3-D moment invariants. IEEE Trans Med Imaging 2007;26(9):1270–82.
(6) Schuldhaus D, Spiegel M, Redel T, Polyanskaya M, Struffert T, Hornegger J, et al. 2D vessel segmentation using local adaptive contrast enhancement. Bildverarbeitung für die Medizin 2011;2011:109–13.
(7) Kirbas C, Quek F. A review of vessel extraction techniques and algorithms. ACM Comput Surv (CSUR) 2004;36(2):81–121.
(8) Chwialkowski MP, Ibrahim YM, Li HF, Peshock RM. A method for fully automated quantitative analysis of arterial flow using flow-sensitized MR images. Comput Med Imaging Graph 1996;20(5):365–78.
(9) Tozaki T, Kawata Y, Niki N, Ohmatsu H, Moriyama N. 3-D visualization of blood vessels and tumor using thin slice CT images. In: Nuclear science symposium and medical imaging conference. IEEE conference record, 1994, vol. 3; 1995. p. 1470–4.
(10) Kawata Y, Niki N, Kumazaki T. An approach for detecting blood vessel diseases from cone-beam CT image. In: International conference on image processing, vol. 2; 1995. p. 500–3 [1995, October].
(11) Eberly D, Gardner R, Morse B, Pizer S, Scharlach C. Ridges for image analysis. J Math Imaging Vis 1994;4(4):353–73.
(12) Bullitt E, Aylward SR. Analysis of time-varying images using 3D vascular models. In: Applied imagery pattern recognition workshop; 2001, October. p. 9–14.
(13) Higgins WE, Spyra WJT, Ritman EL. Automatic extraction of the arterial tree from 3-D angiograms. In: Annual international conference of the IEEE engineering in engineering in medicine and biology society; 1989. p. 563–4 [1989, November].
(14) O'Brien JF, Ezquerra NF. Automated segmentation of coronary vessels in angiographic image sequences utilizing temporal, spatial, and structural constraints. Int Soc Opt Photonics Vis Biomed Comput 1994:25–37.
(15) Prinet V, Mona O, Rocchisani JM. Multi-dimensional vessels extraction using crest lines. In: IEEE 17th annual conference in engineering in medicine and biology society, vol. 1; 1995, September. p. 393–4.
(16) Armande N, Montesinos P, Monga O, Vaysseix G. Thin nets extraction using a multi-scale approach. Comput Vis Image Underst 1999;73(2):248–57.
(17) Sato Y, Nakajima S, Atsumi H, Koller T, Gerig G, Yoshida S, et al. 3D multi-scale line filter for segmentation and visualization of curvilinear structures in medical images. In: CVRMed-MRCAS'97; 1997, January. p. 213–22.
(18) Mao F, Ruan S, Bruno A, Toumoulin C, Collorec R, Haigron P. Extraction of structural features in digital subtraction angiography. In: Proceedings of the 1992 international in biomedical engineering days; 1992. p. 166–9 [1992, August].
(19) Eiho S, Qian Y. Detection of coronary artery tree using morphological operator. In: Computers in cardiology 1997; 1997, September. p. 525–8.
(20) McInerney T, Terzopoulos D. Deformable models in medical image analysis: a survey. Med Image Anal 1996;1(2):91–108.
(21) Chan RC, Karl WC, Lees RS. A new model-based technique for enhanced small-vessel measurements in X-ray cine-angiograms. IEEE Trans Med Imaging 2000;19(3):243–55.
(22) Petrocelli RR, Elion JL, Manbeck KM. A new method for structure recognition in unsubtracted digital angiograms. In: Proceedings of computers in cardiology 1992; 1992, October. p. 207–10.
(23) O'Donnell T, Gupta A, Boult T. A new model for the recovery of cylindrical structures from medical image data. In: CVRMed-MRCAS'97; 1997, January. p. 223–32.
(24) Tolias Y, Panas SM. A fuzzy vessel tracking algorithm for retinal images based on fuzzy clustering. IEEE Trans Med Imaging 1998;17(2):263–73.
(25) Hu S, Hoffman E, Reinhardt JM. Automatic lung segmentation for accurate quantitation of volumetric X-ray CT images. IEEE Trans Med Imaging 2001;20(6):490–8.
(26) El-Baz A, Elnakib A, Khalifa F, El-Ghar MA, McClure P, Soliman A, et al. Precise segmentation of 3-D magnetic resonance angiography. IEEE Trans Biomed Eng 2012;59(7):2019–29.

(27) Benmansour F, Cohen LD. Tubular structure segmentation based on minimal path method and anisotropic enhancement. Int J Comput Vis 2011;92(2):192–210.
(28) Li H, Yezzi A. Vessels as 4-D curves: global minimal 4-D paths to extract 3-D tubular surfaces and centerlines. IEEE Trans Med Imaging 2007;26(9):1213–23.
(29) Angiograms PCMR. Vessel and aneurysm reconstruction using speed and flow coherence information in phase contrast magnetic resonance angiograms. Doctoral dissertation, University of Oxford, United Kingdom; 2001.
(30) Hao J, Li M. A supervised bayesian method for cerebrovascular segmentation. WSEAS Trans Signal Process 2007;3(12):487–95.
(31) Sen Y, Zhang Y, Qian Y, Morgan M. Investigation of image segmentation methods for intracranial aneurysm haemodynamic research. Modell Med Biol X 2012;17:259.
(32) Bogunović H, Pozo JM, Villa-Uriol MC, Majoie CB, van den Berg R, van Andel HAG, et al. Automated segmentation of cerebral vasculature with aneurysms in 3DRA and TOF-MRA using geodesic active regions: an evaluation study. Med Phys 2011;38(1):210–22.
(33) Linden A. Measuring diagnostic and predictive accuracy in disease management: an introduction to receiver operating characteristic (ROC) analysis. J Eval Clin Pract 2006;12(2):132–9.
(34) THROMBUS*. A quantitative model of thrombosis in intracranial aneurysms. (*THROMBUS project is a collaborative project funded by the European Commission in the Seventh Framework Programme. The project is funded for 3 years: from 01-02-2011 to 31-01-2014); 2011.
(35) Uchiyama Y, Yokoyama R, Ando H, Asano T, Kato H, Yamakawa H, et al. Computer-aided diagnosis scheme for detection of lacunar infarcts on MR images. Acad Radiol 2007;14(12):1554–61.
(36) Arimura H, Magome T, Yamashita Y, Yamamoto D. Computer-aided diagnosis systems for brain diseases in magnetic resonance images. Algorithms 2009;2(3):925–52.
(37) Shiraishi J, Li Q, Appelbaum D, Doi K. Computer-aided diagnosis and artificial intelligence in clinical imaging. Semin Nucl Med 2011;41(6):449–62, November.
(38) Albatal R, Mulhem P, Chiaramella Y, Chin TJ. Comparing image segmentation algorithms for content based image retrieval systems; 2009.